JJMIE

Volume 11 Number 4, December. 2017
ISSN 1995-6665
Pages 225 -233

Jordan Journal of Mechanical and Industrial Engineering

Transevaporative Cooling Performance of a Three-Sided Wind Catcher

M.N. Khan [a] , I. Janajreh [*b]

[a] Dept. of Mechanical and Materials Engineering, Masdar Institute of Science and Technology, Abu Dhabi, United Arab Emirates
[b] Dept. of Mechanical and Materials Engineering, Khalifa University of Science and Technology, Abu Dhabi, United Arab Emirates,

Abstract

A wind catcher is a structure used for capturing wind at higher elevations and directing it to the desired locations for cooling. A down-draft evaporative wind catcher uses the principle of evaporative cooling to provide passive cooling as well as natural ventilation. The present paper presents the performance of a three-sided wind catcher at Masdar city, subjected to mist injection. The 45 m tall wind catcher is modelled for different wind speeds ranging from 1-5 m/s using computational fluid dynamics. The numerical model accounts for Eulerian-Lagrangian formulation. Equations of continuity, momentum and energy along with realizable k-ε turbulence model are employed to calculate the flow field. Droplet evaporation in discrete phase model is used for tracking the liquid water mists. The results demonstrate that the wind catcher performance is greatly influenced by the external wind speed. Higher wind speed resulted in higher rate of evaporation and lower air temperatures. The density, water vapour mass fraction and the relative humidity increases as the air flow travel downwards to the wind catcher exit. While the temperature decreases significantly in the downward direction of the wind catcher. The present study shows the promise of using the computational models in analysing and optimizing the design and performance of the wind catcher.

1. Introduction

Refrigeration and cooling techniques, like the free cooling technique [1] and evaporative cooling, are used for energy efficiency. Evaporative cooling method for passive cooling and air conditioning of the buildings has been in practice since olden days in dry climatic regions, such as Middle Eastern countries. Various types of designs and configurations have been used, such as spraying the walls with water or building a special structure to capture the wind and passing through moist surfaces for cooling [2-3]. Detailed description can be found elsewhere [4]. Wind catcher structures have been given different names in different regions. They are called Badinge in Syria, Baud-geers in Iran and Burjeel in gulf region. Wind catchers are the structures which have been used to provide passive cooling and natural ventilation. These towers are designed to catch the wind at higher elevations and direct them to the desired spaces [4]. The simplest form of the tower provides sensible cooling while evaporative cooling occurs when water is introduced into the system [5]. Evaporative cooling results in reduction in temperature from evaporation of a liquid. It is due to the removal of latent heat from the hot incoming air. This could be integrated in the wind catcher system by using different techniques, such as the mist spray, wetted clay columns, wetter mats etc. Good ventilation along with cooling is desired for indoor spaces. The wind speeds greatly influence the ventilation since high wind speeds provide high air flow rate. The air flow inside the wind catcher is greatly influenced by the wind speed, ambient temperature, atmospheric relative humidity, amount of water added when evaporative cooling is desired and the geometry of the wind catcher (cross-sectional area, height of the tower etc.) All these parameters have to be studied in detail in order to obtain an optimized performance of the wind catcher.

Several experimental evaluations have been performed on various kinds of wind catcher designs. Elmualim [6] conducted an experimental investigation of the performance of square and circular cross-section wind catchers in a wind tunnel. Pressure coefficients, air speed and volumetric flow rates were measured. A Computational Fluid Dynamic (CFD) investigation based on the experiments has also been performed to obtain the pressure distribution and air flow pattern in and around wind catcher. It was observed that the performance of the wind catcher depends mainly on the speed and the wind direction. It was also reported that ventilation rate increases as the velocity of air increases.

Kirk and Kolokotroni [7] conducted air-exchange tests and reported that both wind and stack-effect influences air exchange rate through the buildings. Su and Riffat [8] conducted the flow rate measurements for various wind speeds in a mono-draught wind catchers. The effect of

* Corresponding author e-mail: ijanajreh@masdar.ac.ae.

varying the room pressure on the supply and extract flow rate from the openings of the room had also been studied and the effect is found to be quite large at low wind speeds. Bahadori *et al*. [9] measured pressure coefficients in the wind catchers to evaluate the air flow pattern. Wind catchers are ongoing topic of interests for the reduction and implementation of efficient air conditioning at lower energy penalty for building. Designing an efficient wind catcher system for different climatic conditions is a difficult task. A study was conducted by Dehghani-sanij *et al.* [10]. A new efficient wind catcher system has been designed and tested in real conditions. The advantages of the wind catcher system were demonstrated. However, the experimental studies of wind catcher systems are costly and very difficult. The assessment of wind catcher using CFD is very important for performance evaluation and improvements in the system design.

CFD has been widely used to study the air flow in and around buildings [11], since it can provide detailed distribution of airflow velocity, temperature, pressure and humidity. The results obtained have been approved useful for applications of cooling, ventilation and low rise structural loading [12] as well permeable screen structural loading and for building code revisions [13]. Significant literature is available on such studies based on different climatic conditions and design of the wind catcher system. Kalantar [14] conducted a numerical study of the cooling performance of a wind catcher in a hot and dry region of Yazd in Iran. The results obtained complement the promise of evaporative cooling in a hot and dry region particularly when wind catcher is equipped with the water spray system. Saffari and Hosseinnia [15] used a two-phase Euler-Lagrange model to investigate the performance of a new wind catcher design. The design consists of wetted columns with wetted curtains hung in the tower. The effect of water droplet temperature and its diameter, wind velocity, temperature and relative humidity had been investigated. It was reported that wetted columns with 10 m height decreases the ambient air temperature significantly by 12^{o} C and increases its relative humidity by 22%.

The present authors, in a recent work, numerically assessed trans-evaporative cooling in providing occupants comfort in two-level simple dwelling in arid region [16]. Limited studies have addressed the three sided wind catcher in hot and humid climatic conditions. In the present study, the performance of the three sided wind catcher at the Masdar City, Abu Dhabi has been investigated numerically (see Fig. 1). The wind catcher is situated in the middle of an open top court connected with narrow corridors. The wind catcher helps in lowering the temperature down to reasonable range during hot summer. Temperatures and relative humidity in Abu Dhabi can reach as high as 45 °C and 27-80%, respectively. Hence, it is a challenge to use a wind catcher that can lower the air temperature while maintaining the relative humidity in comfort zone. On the other hand, wind speeds range from 4-7 m/s which is a favorable point. The column of the wind catcher is in the form of slightly converging-diverging tube in which the added evaporative fluid mass helps in accelerating the incoming air velocity at the exit of the wind catcher providing excellent air flow pattern in the court. The cooling output from the wind catcher is heavily dependent on the wind speed as it affects the heat and mass transfer characteristics. Hence, the performance of the wind catcher under different wind speeds has been evaluated.

2. Description of the Wind Catcher

Generally, wind catchers are installed on the roof top of the buildings, but they also used in providing the cooling effect to the semi-enclosed spaces. The 45 m long Masdar City wind tower is a three-sided wind catcher with a circular cross-section and is used to provide cooling in an open-top court yard of nearly 20m × 20m. The schematic of the wind tower is shown in Fig. 1. The diameter of the tower varies from top to bottom with a mean diameter of 4.9 m. It is mounted in steel frame structure at the top of which there are nine louvers on each side, which opens in the direction of the prevailing wind and closes or adjusted in other directions to trap the maximum amount of wind. The wind then flows down into an impermeable column made of Polytetrafluoroethylene (PTFE) membrane that directs the wind down to the court yard. For evaporative cooling, mist generators are employed at the tower top entry. Depending on the temperature, humidity and wind speed, the mist generators can add evaporative cooling to the air.

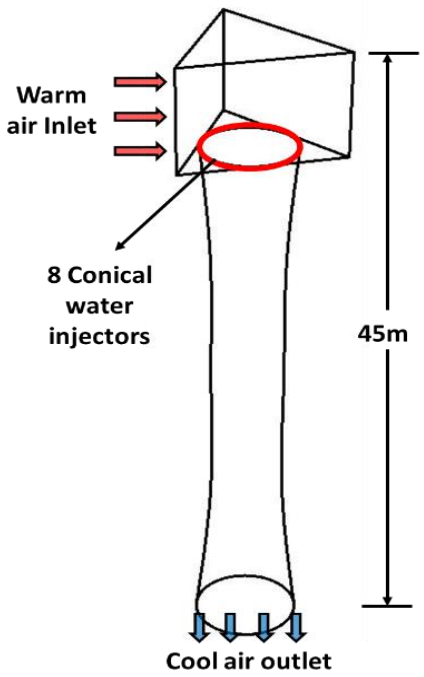

Fig. 1: Schematic of the three sided wind catcher at Masdar City

3. Computational Fluid Dynamic Modeling

3.1. Geometry

The three-dimensional geometrical model, based on the aforementioned dimensions, is presented in Fig. 2. The overall numerical domain size is 110m × 60m × 40m and bounded by two sided far fields, incoming velocity (S1) and exit pressure (S4), ground (represented by black

surface) and top symmetry. The air flows through the velocity inlet (S1) and exit the domain through the pressure outlet (S4). It is assumed that air is entering the wind catcher from only one fully open side (S2) louvers and the other two side louvers are closed. The outlet of the wind catcher is about 3m above the ground. The ground is made of concrete and is represented as no-slip wall in Fig. 2. The water injectors are introduced at the very top entrance of the converging-diverging section of the wind catcher before it is driven in the downward direction. This will ensure that the water droplets experience higher residence time in contact with the air and eventually reducing the air temperature.

3.2. Governing Equations

In the Eulerian-Lagrangian approach, the air flow is considered a continuous phase using the Eulerian formulation whereas the water droplets and their trajectories are considered a discrete phase using the Lagrangian formulation. Flow field is three dimensional, turbulent, non-isothermal and incompressible in nature.

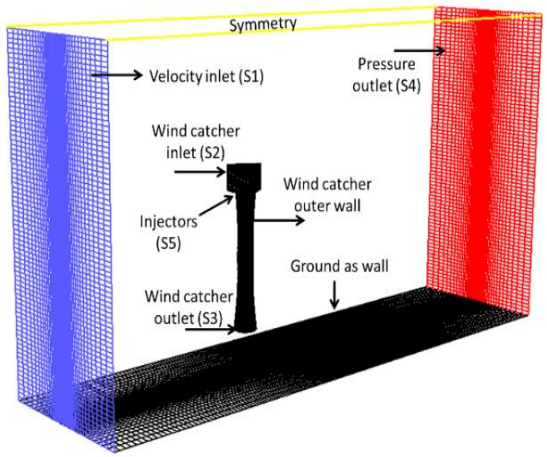

Fig. 2: Geometry and computational domain

The following are the governing equations for continuous (air) and discrete (water) phases and their sub-modeling scalar transport equations.

3.2.1. Continuous Phase (Air)

Continuity Equation

$$\frac{\partial(\rho u_i)}{\partial x_i} = S_m \quad (1)$$

where ρ is the moist air density (kg/m^3), u_i is the velocity vector (m/s) and S_m is the mass source term (kg/s·m^3) which is added or removed from the continuous phase due to evaporation or condensation of the water droplets.

Momentum Equation

$$\frac{\partial}{\partial x_i}(\rho u_i u_j) = \frac{\partial p}{\partial x_j} + \frac{\partial}{\partial x_j}\left[\mu\left(\frac{\partial u_i}{\partial x_j} + \frac{\partial u_j}{\partial x_i}\right)\right] + \frac{\partial}{\partial x_j}\left(-\rho\overline{u_i' u_j'}\right) + f_i \quad (2)$$

Boussinesq hypothesis has been employed to relate the Reynolds stresses $\left(\rho\overline{u_i' u_j'}\right)$ to the mean velocity gradient, p is the static pressure (Pa), μ is the dynamic viscosity (Pa·s) and f_i is the external body force in j^{th} direction (N/m^3).

Energy Equation

$$\frac{\partial}{\partial x_j} u_i(\rho E + p) = \frac{\partial}{\partial x_j}\left[\left(\gamma + \frac{C_{pa}\mu_t}{Pr_t}\right)\frac{\partial T}{\partial x_j} - \sum_j h_j J_j\right] + S_h \quad (3)$$

where γ is the thermal conductivity of the fluid (W/m·K), c_{pa} is the specific heat of air at constant pressure (J/kg·K), μ_t is the turbulent viscosity (Pa·s), Pr_t is the turbulent Prandtl number, T is the temperature (K), h_j is the enthalpy of the species (J/kg), J_j is the diffusion flux of species j (kg/m^2·s) and S_h is any volumetric source. The term E is defined as follows:

$$E = \sum h_j Y_j + \frac{u^2}{2} \quad (4)$$

where Y is the species mass fraction

Species Transport Equation

Species transport equation of water vapor mass fraction (Y_{H2O}) into air can be defined as follows:

$$\frac{\partial}{\partial x_j}\left(\rho Y_{H_2O} u_i\right) = \frac{\partial}{\partial x_j}\left[\left(\rho D_{H_2O} + \frac{\mu_t}{Sc_t}\right)\frac{\partial Y_{2O}}{\partial x_j}\right] + S_{H_2O} \quad (5)$$

where D_{H2O} is the diffusion coefficient of water vapor into air (2.88 ×10^{-5}), S_{ct} is the turbulent Schmidt number (0.7) and S_{H2O} is the water vapor added to or removed from the air due to evaporation or condensation.

Turbulent Scalar Equations

The turbulent kinetic energy is written as:

$$\frac{\partial}{\partial x_i}(\rho k u_i) = \frac{\partial}{\partial x_j}\left[\left(\mu + \frac{\mu_t}{\sigma_k}\right)\frac{\partial k}{\partial x_j}\right] + G_k + G_b - \rho\varepsilon - Y_M + S_k \quad (6)$$

and the turbulent dissipation rate is expressed as:

$$\frac{\partial}{\partial x_i}(\rho\varepsilon u_i) = \frac{\partial}{\partial x_j}\left[\left(\mu + \frac{\mu_t}{\sigma_\varepsilon}\right)\frac{\partial \varepsilon}{\partial x_j}\right] + \rho C_1 S_\varepsilon - \rho C_2 \frac{\varepsilon^2}{k+\sqrt{\nu\varepsilon}} + C_{1\varepsilon}\frac{\varepsilon}{k} C_{3\varepsilon} G_b \quad (7)$$

where k is the turbulent kinetic energy (m^2/s^2), ε is the turbulent dissipation rate (m^2/s^3), σ_k and σ_ε are the turbulent Prandtl numbers for k and ε , respectively, G_k and G_b represents the generation of turbulent kinetic energy due to the mean velocity gradients and buoyancy, respectively, Y_m here is the contribution of the fluctuating dilation in compressible turbulence to the overall dissipation rate, C_s are the constants and S is the source term.

The species transport equation and the turbulent scalar equations are applied to the continuous phase only. On the other hand, the liquid droplets are formulated as discrete particles. The species transport equation is used for the air and the water mass fraction within the air after evaporation takes place. As the velocity is significantly high, the Reynolds number for the continuous phase falls in turbulent region. Better mixing, high heat and mass transfer occurs during turbulence and hence, it should be taken into account in order to accurately predict the wind

catcher performance. Therefore, the realizable k-epsilon turbulent model is employed that takes care of turbulence.

3.2.2. Discrete Phase (Water)

Water Droplet Trajectory Calculations

In the Lagrangian formulation, the water droplet velocity is related to the rate of change of droplet position. The trajectory is predicted by using the force balance on the droplet which equates the particle inertia with the forces acting on the particle and can be written as:

$$\frac{du_p}{dt} = F_D(u - u_p) + \frac{g(\rho_p - \rho)}{\rho_p} + F_x \quad (8)$$

here u is the moist air velocity (m/s), u_p is the droplet velocity (m/s), $F_D(u\text{-}u_p)$ is the drag force per unit droplet mass, g is the gravitational acceleration (m/s^2), ρ_p is the droplet density (kg/m^3), ρ is the moist air density (kg/m^3) and F_x is the additional forces added as the source terms:

$$F_D = \frac{18\mu}{\rho_P d_p^2}\frac{C_D Re}{24} \quad (9)$$

$$C_D = a_1 + \frac{a_2}{Re} + \frac{a_3}{Re^2} \quad (10)$$

$$Re = \frac{\rho d_p |u_p - u|}{\mu} \quad (11)$$

where d_p is the droplet diameter (m), C_D is the drag coefficient, Re is the Reynolds number and a_1, a_2 and a_3 are constants.

Heat and Mass Transfer Calculations

Inside the wind catcher, the heat is transferred from the hot surrounding air into the water droplet by convection and evaporation. The heat transfer due to radiation is neglected in this study. The heat balance relating the droplet temperature to the convective heat transfer is given as:

$$m_p c_{pw}\frac{dT_p}{dt} = hA_p(T_\infty - T_p) \quad (12)$$

where m_p is the droplet mass (kg), c_{pw} is the water droplet heat capacity (J/kg·K), A_p is the droplet surface area (m^2), T_∞ is the local temperature of the continuous phase (K), h is the convective heat transfer coefficient (W/m^2·K) and T_p is the droplet temperature (K).

The droplet temperature at the next time step is calculated by integrating the above equation and is as follows:

$$T_p(t + \Delta t) = T_\infty + \left(T_p(t) - T_\infty\right)e^{(-A_p h/m_p c_p)\Delta t} \quad (13)$$

where Δt is the integration time step

The heat transfer coefficient (h) is calculated using the correlation of Ranz and Marshall [17]:

$$Nu = \frac{hd_p}{k_\infty} = 2.0 + 0.6Re_d^{1/2}Pr^{1/3} \quad (14)$$

where Nu is the Nusselt number, k_∞ is the thermal conductivity of the continuous phase (W/m·K), Re_d is the Reynolds number based on the droplet diameter and the relative velocity and Pr is the Prandtl number of the continuous phase.

The rate of vaporization of water by air is related to the gradient of the vapor pressure between the droplet surface and the main air stream and is given as follows:

$$\frac{dm_p}{dt} = A_p\frac{h_m}{R}\left(\frac{P_{sat}(T_p)}{T_p} - C\frac{p}{T_\infty}\right) \quad (15)$$

where h_m is the mass transfer coefficient (m/s), R is the universal gas constant (J/mol·K), P_{sat} is the saturated vapor pressure and C is the vapor concentration (kmol/m^3).

The mass transfer coefficient is calculated from Sherwood number (Sh) correlation:

$$Sh = \frac{h_m d_p}{D_{va}} = 2.0 + 0.6Re_d^{1/2}Sc^{1/3} \quad (16)$$

where D_{va} is the diffusion coefficient of vapor in the bulk (m^2/s), Sc is the Schmidt number.

Therefore, the droplet mass is reduced according to the relation:

$$m_p(t + \Delta t) = m_p(t) - A_p\frac{h_m}{R}\left(\frac{P_{sat}(T_p)}{T_p} - C\frac{p}{T_\infty}\right) \quad (17)$$

Now, the droplet temperature is updated based on the heat balance relation between the sensible heat change in the droplet and the convective and evaporative heat transfer between the droplet and the air:

$$m_p c_{pw}\frac{dT_p}{dt} = hA_p(T_\infty - T_p) + \frac{dm_p}{dt}h_{fg} \quad (18)$$

where h_{fg} is the latent heat of vaporization (J/kg).

3.2.3. Coupling between Air and Water Phases

Along with the droplet trajectory calculations, the heat, mass and momentum gained or lost by the droplet that follows the trajectory are also calculated and these quantities are incorporated as the source terms in the respective equations in the subsequent continuous phase calculations. The momentum, mass and heat exchanges are given as:

$$F = \sum\left(\frac{18\mu}{\rho_P d_p^2}\frac{C_D Re}{24}(u - u_p) + F_{other}\right)\frac{dm_p}{dt}\Delta t \quad (19)$$

$$M = \frac{\Delta m_p}{m_{p,0}}\dot{m}_{p,0} \quad (20)$$

$$Q = \left[\frac{m_{p,av}}{m_{p,0}}c_{pw}\Delta T_p + \frac{\Delta m_p}{m_{p,0}}\left(-h_{fg} + \int_{T_{ref}}^{T_p} c_{pv}dT\right)\right]\dot{m}_{p,0} \quad (21)$$

where F_{other} are other interaction forces, c_{pw} is the heat capacity of the water droplet (J/kg·K), c_{pv} is the heat capacity of the water vapor (J/kg·K), $\dot{m}_{p,0}$ is the initial mass flow rate of the droplet injection (kg/s), $m_{p,0}$ is the initial mass of the droplet (kg), $m_{p,av}$ is the average mass of the droplet in the cell (kg), T_{ref} is the reference temperature (K), ΔT_p is the change in temperature (K) and Δm_p is the change in mass of the droplet (kg).

3.3. Boundary Conditions

The flow is considered as incompressible [11] since the wind speed is varied from 1-5 m/s and is specified at the velocity inlet (S1). As this speed is not constant at every height, a power law for wind speed is adopted to create a velocity gradient. The wind profile power law [17] is a relationship between the wind speeds at one height, and

those at another. In order to estimate the wind speed at a certain height x, the relationship would be rearranged to:

$$u_x = u_r \left(\frac{z_x}{z_r}\right)^{\alpha} \quad (22)$$

where u_x is the wind speed (m/s) at height z_x (m), and u_r is the known wind speed at a reference height z_r. The exponent (α) is an empirically derived coefficient that varies dependent upon the stability of the atmosphere. For neutral stability conditions or terrain category, α is approximately 0.11 [19].

The outflow of the computational domain is specified as pressure outlet (S4) and is set at a reasonable distance to ensure that the solution near the wind catcher is not affected by the backflow conditions. The openings S2 and S3 in Fig. 2 are the inlet and outlet of the wind catcher, respectively.

Mist is introduced through eight conical injections which are defined and equally distributed circumferentially at position S5. Droplet evaporation has been considered with uniform droplet diameter distribution. The droplet diameter is assumed as 40 μm with a cone angle of 60°. The water is sprayed at a rate of 0.1 kg/s with a velocity of 45 m/s and temperature 298 K. The water droplets have been assumed to have inelastic collisions with the walls of the wind catcher. Hence, the reflected water droplet will have only tangential component of the momentum.

3.4. Domain Discretization and Solution

The grid consists of an unstructured volume mesh with rectangular meshes on the surface of the geometry. The total number of cells in the grid is 959,306 with 1,975,876 faces and 197,041 nodes. The maximum and minimum grid volumes are 0.000126 m^3 and 3.99 m^3, respectively.

This solution was carried using the commercial CFD code FLUENT based on finite volume approach. Segregated solver which provides good robustness has been used. Reynold-Averaged Navier-Stokes (RANS) equations with the constitutive eddy viscosity realizable k-ε turbulence model is solved with Boussinesq hypothesis and discrete phase injections. The Semi-Implicit Method for Pressure-Linked Equations (SIMPLE) algorithm is chosen for pressure-velocity coupling and second order upwind discretization scheme is employed for spatial derivatives. The convergence criterion is set at 0.00001 residual for the continuity, and three momentums and energy scalar equations.

4. Results and Discussions

The simulations are performed for three wind velocities, ranging from 1 m/s to 5 m/s. The wind catcher is assumed to be situated in an open space in the present study. In summer, the weather in Abu Dhabi is extremely hot and humid. The ambient temperature may reach as high as 323K whereas the relative humidity can vary anywhere between 40-50%. The wind speed also can vary between 2 m/s to about 7 m/s. This presents a challenge in utilizing the evaporative cooling technique using a wind catcher. The results at the wind speed of 3 m/s are discussed here as it is the average wind speed in summer. Fig. 3 shows the contour of velocity at a central plane parallel to the direction of the wind. It can be seen in Fig. 3 that the air velocity increases to about 7 m/s inside the column of the wind catcher. It is due to the additional evaporated mist that changes phase and expands within the wind catcher duct. At the exit, the air velocity reduces to about 4 m/s which is suitable for a semi-enclosed space. Fig. 4 represents the distribution of temperature in and around the wind catcher. It can be observed that due to the evaporative cooling, the hot air inside the wind catcher cools down to about 300 K. The reduction in temperature takes place near the walls in line with the liquid water injectors in the downward direction. The air at the center of the column takes relatively longer to cool down. The obtained average temperature at the exit of the wind catcher is about 303 K which means that a reduction of 10 K in the air temperature is achieved. This temperature of the air is considered comfortable in the semi-enclosed spaces. Fig. 5 shows the relative humidity distribution. An average relative humidity of about 44% is considered initially. As can be seen in the contour, the relative humidity reaches over 100% along the walls, implying that the air is fully saturated near the walls. The average relative humidity at the wind catcher exit is about 80% which is very high and beyond the comfort zone. However, as the air travels out of the wind catcher, the relative humidity further reduces after mixing with the less humid surrounding air. To avoid high humid conditions, there should be a provision to condense the water vapor which eventually reduces the relative humidity to the comfortable range. The most appropriate solution to the above problem would be to place a fine mesh made of hydrophilic material at the wind catcher exit which would help in condensing the excess water vapor from the air.

From the above results, it is evident that the behavior of the humid air inside the wind catcher column is highly non-uniform in both radial and axial directions. In the present study, the changes in humid air behavior at the center line of the wind catcher column are studied. Figs. 6-12 depicts the humid air behavior in terms of air velocity, static pressure, density, evaporated water mass, water mass fraction, relative humidity and temperature.

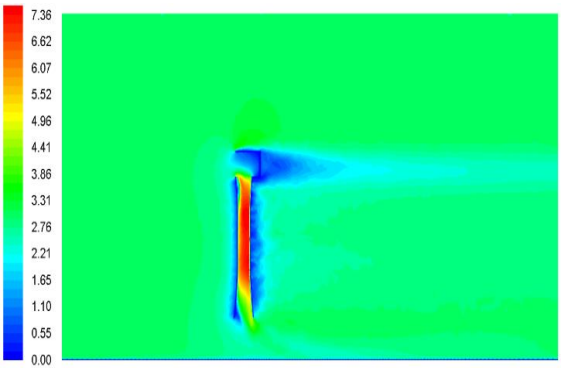

Fig. 3: Velocity contour at a wind speed of 3 m/s

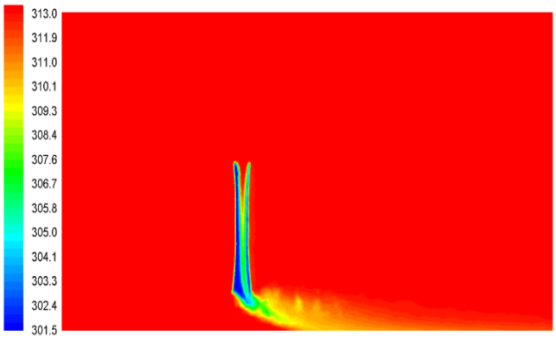

Fig. 4: Temperature contour at a wind speed of 3 m/s

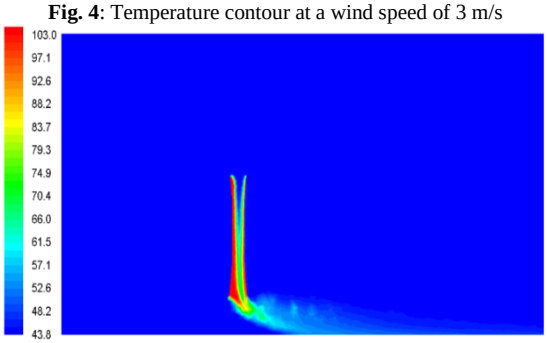

Fig. 5: Relative humidity contour at a wind speed of 3 m/s

Fig. 6 shows the variation of velocity from the entrance to the exit of the wind catcher for three inlet wind speeds ranging from 1-3 m/s. The trend in all the three cases is similar. Injection water through mist sprays result in absorption of water by the hot air making it heavier, denser and more humid. Consequently, the velocity increases due to the increase in negative buoyancy force. In addition, the converging-diverging design will also have an effect on the fluid velocity. The decrease in cross-sectional area at the middle also aids in velocity increase to satisfy the mass conservation. The velocities, then decrease as the dense air moves towards the wind catcher exit. As expected, the high inlet wind speeds resulted in high air velocities inside the wind catcher.

Fig. 7 shows the change of pressure from the entrance to the exit of the wind catcher column. The trend is opposite to that followed by the velocity in Fig. 6. An increase in velocity of the fluid particle would result in decrease in its pressure. High wind speeds produces lower static pressures inside the wind catcher. Nevertheless, the difference in pressure at the wind catcher exit is very small and can be considered negligible.

The fluctuation in density along the center line of the wind catcher is shown in Fig. 8. As water is sprayed in the incoming air, the air will become heavier due to absorption of liquid water droplets. Therefore, the density increases as the air flows towards the exit. High wind speeds bring in large volumes of air inside the wind catcher. Hence, as a result, more and more water can be absorbed resulting in high densities as shown in Fig. 8. The fluctuations are observed due to the fact that the absorption of water is not uniform throughout the wind catcher column. The water is sprayed in the downward direction near the wall and has less pronounced effect at the center line. Hence, the variation in center line density is not smooth. Another thing to be noticed is that the density at the exit for inlet wind speeds higher than 3 m/s is similar.

Fig. 9 represents the mass flow rate of water that is evaporated along the center line. It can be seen that for low wind speeds, the rate of evaporation is more in the bottom half of the column. This is due to the increase in fluid velocities. On the other hand, the rate of evaporation is high in the upper half of the column for high wind speeds and it reduces as the flow travel towards the exit. This is due to the fact that significant absorption has already occurred which, consequently, cools down the air and reduces its temperature significantly and hence, the rate of evaporation is low. High wind speeds create a forced convection situation which ultimately affects the rate of evaporation, relative humidity and the air temperature.

In Fig. 10, the axial mass fraction of water vapor in the air at the center line of the wind catcher column is presented. The results show that mass fraction increases as the air flow reaches the wind catcher exit. High wind speeds capture more water vapor and hence, get saturated very quickly. Again, the fluctuations are due to the non-uniform behavior of the fluid particles inside the column.

Fig. 11 shows the axial relative humidity at the center line of the wind catcher column. The relative humidity reaches almost 100% for high wind speeds and about 70% for the lowest wind speed (1 m/s) as shown in the figure. These high values of relative humidity are out of comfortable criteria. Hence, as mentioned earlier, provisions have to be made in order to capture the water vapor from the air without increasing the air temperature. A mesh made of hydrophilic material can be used at the wind catcher exit to capture the water vapor from the air.

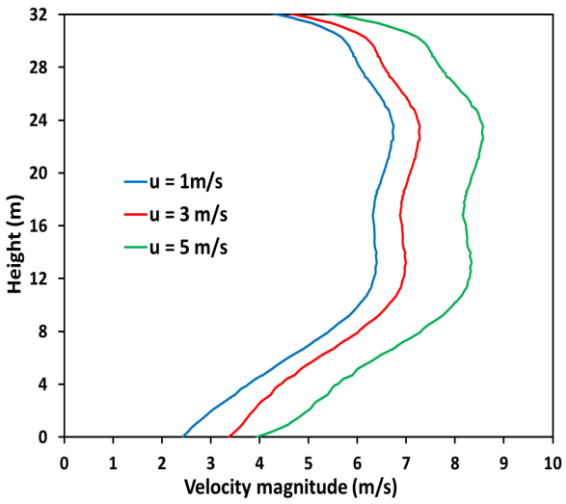

Fig. 6: Variation of air velocity from entrance to exit

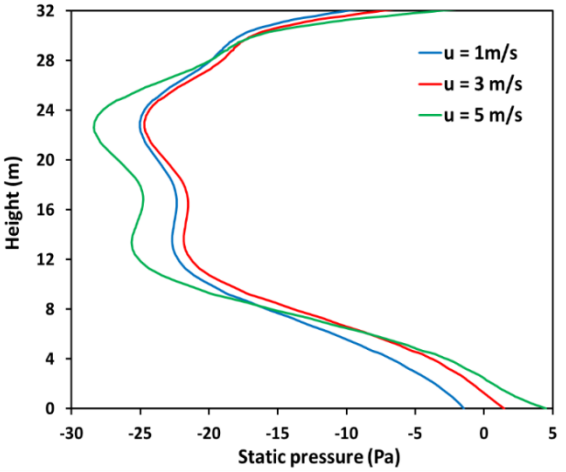

Fig. 7: Variation of pressure from entrance to exit

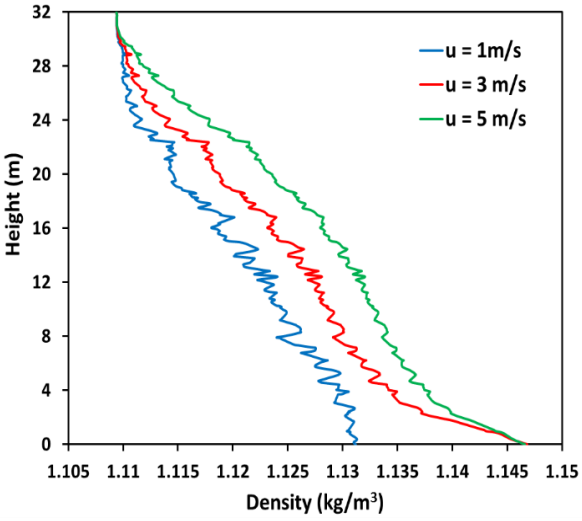

Fig. 8: Variation of density from entrance to exit

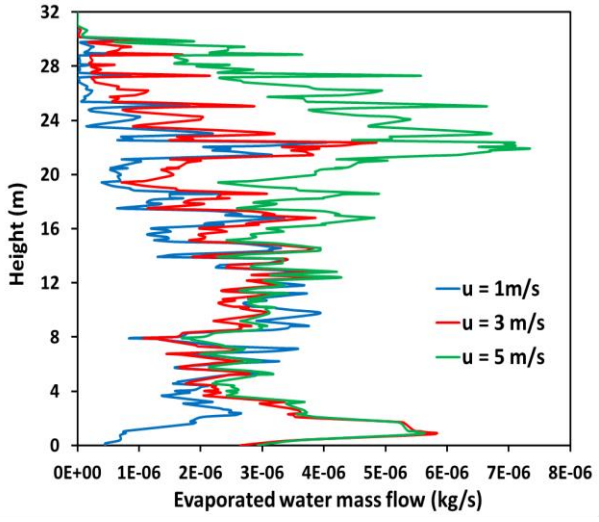

Fig. 9: Variation of evaporated water mass from entrance to exit

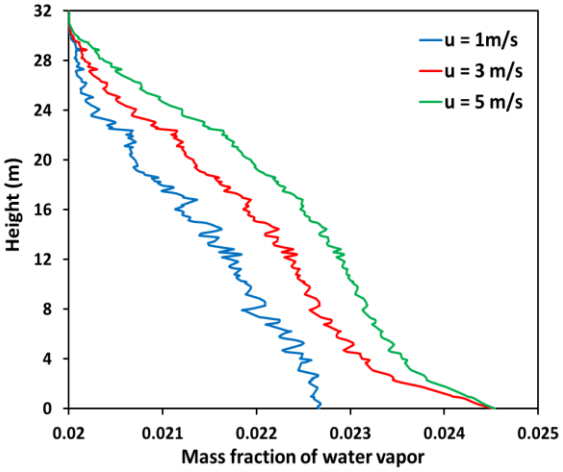

Fig. 10: Variation of water mass fraction from entrance to exit

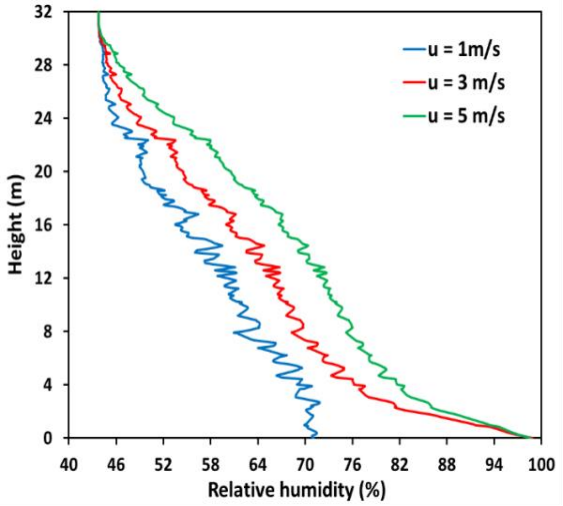

Fig. 11: Variation of relative humidity from entrance to exit

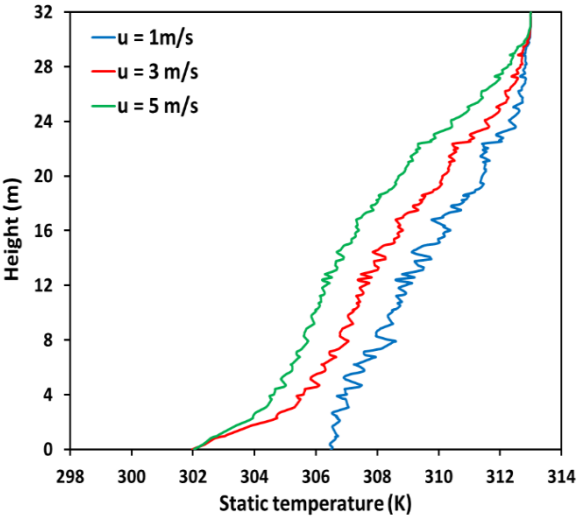

Fig. 12: Variation of temperature from entrance to exit

Table 1: Parameters at various wind speeds

Wind speed (m/s)	1	3	5
Pressure (Pa)	-1.138	-0.122	1.228
Density (kg/m^3)	1.136	1.142	1.143
Velocity (m/s)	2.86	3.357	3.81
Temperature (K)	304.83	303.28	302.9
Water mass fraction	0.0233	0.0241	0.0242
Relative humidity (%)	81.61	91.18	93.02

The variation in the air temperature for different velocities is shown in Fig. 12. The results show that high wind speeds resulted in low exit temperatures. The temperature is reduced significantly to 302K, which is about 11K reduction. This can be attributed to the absorption of heat during evaporative cooling process.

In addition to the humid air behaviour along the centre line of the wind catcher column, the state of the humid air at the exit is critical to the overall performance of the wind catcher. The parameters discussed above are averaged over the cross-sectional area at the wind catcher exit and are listed in Table 1. It can be observed that the pressure, density, velocity, water mass fraction and relative humidity increase with increasing inlet wind speeds. On the other hand, the air temperature decreases with increasing inlet wind speeds. This emphasizes the fact that the performance of the wind catcher is greatly influenced by the ambient wind speeds.

The main parameters that are to be controlled in order to achieve desirable outlet temperature are mass flow rate of water, the cone angle, velocity of the spray, diameter of the liquid droplet etc. In the current study, the mass flow rate of water is chosen as 0.1 kg/s such that the temperature is reduced by 10 K. The spray angle of 60° is chosen since results in good distribution of water droplets. The water jet velocity is assumed as 45 m/s since at this velocity fine mist droplets are formed. All the aforementioned parameters are important. However, in order to correctly predict the outlet temperature further simulations is required by varying the above parameters individually.

5. Conclusions

In the present study, a numerical model has been developed to simulate the three sided wind catcher at the Masdar City, Abu Dhabi. The performance of the wind catcher at different wind speeds is analyzed quantitatively. The effect of wind speeds on the velocity, pressure, density, rate of evaporation, water mass fraction, relative humidity and temperature has been studied. The results obtained showed that spraying of liquid water in hot air has significant effect on the aforementioned parameters. The wind catcher is capable of reducing the temperature by 10-12 K at the peak of its performance while keeping the air velocity in comfort range. However, the relative humidity obtained is very high and out of comfortable zone. This is because of the ambient relative humidity which is already high in summer.

The results shows that the higher wind speeds show better performance as they create a forced convection condition resulting in high evaporative cooling. The air velocities inside the wind catcher column increases first due to absorption of the water and then decreases as the air flow proceeds toward the exit as opposed to pressure which increases as the flow moves toward the exit. Due to water absorption, the air becomes moist and heavier and hence, the density increases. Mass fraction of water in the air and consequently, the relative humidity are increased with decrease in the height of the column. The air temperature decreases significantly due to the heat absorption in evaporative cooling.

The only problem associated with the current wind catcher is the exit relative humidity which is beyond the comfort criteria. The most appropriate solution would be to use a mesh made of hydrophilic material that can adsorb the water vapour from the air without increasing its temperature. It is just an idea and more work is needed in order to determine its usefulness and the additional costs it incurs. It is also important to consider the annual weather data of Masdar City. Some of these data are found elsewhere of the authors work [20]. Additionally, validated atmospheric boundary layer wind tunnel flow simulations commensurated with density-, pressure-, temperature-, and humidity-velocity correlation renders the establishment of better guidelines for wind catcher development [21]. This is a research study on its own that will be considered in a future development of the present work. Further investigations based on various other parameters, like the inlet air temperature, relative humidity, the spray water temperature, droplet diameter, spray velocity and liquid water mass flow rate are required in order to assess and optimize the performance of the wind catcher for the climatic conditions of Abu Dhabi.

Acknowledgments

The present study was supported by the Government of Abu Dhabi to help fulfil the vision of the late President Sheikh Zayed Bin Sultan Al Nahyan for sustainable development and empowerment of the UAE and humankind.

References

[1] A. Al-Salaymeh and M.R. Abdelkader, “Efficiency of free cooling technique in air refrigeration systems,” Jordan Journal of Mechanical and Industrial Engineering, vol. 4(6), pp. 711-724, December 2010.

[2] M. Younis, K. Ghali, and N. Ghaddar, “Performance evaluation of the displacement ventilation combined with evaporative cooled ceiling for a typical office in Beirut,” Energy Conversion and Management, vol. 15(105), pp. 655-664, November 2015.

[3] M. Ali, V. Vukovic, N.A. Sheikh, and H.M. Ali, “Performance investigation of solid desiccant evaporative cooling system configurations in different climatic zones,” Energy Conversion and Management, vol. 30(97), pp. 323-339, June 2015.

[4] C. Karakatsanis, M.N. Bahadori, and B.J. Vickery, “Evaluation of pressure coefficients and estimation of air flow rates in buildings employing wind towers,” Solar Energy, vol. 37(5), pp. 363-374, December 1986.

[5] A.A. Badran, “Performance of cool towers under various climates in Jordan,” Energy and Buildings, vol. 35(10), pp. 1031-1035, November 2003.

[6] A.A. Elmualim, and H.B. Awbi, "Wind tunnel and CFD investigation of the performance of "Windcatcher" ventilation systems," International Journal of ventilation, vol. 1(1), pp. 53-64, June 2002.

[7] S. Kirk, and M. Kolokotroni, "Windcatchers in modern UK buildings: experimental study," International Journal of ventilation, vol. 3(1), pp. 67-78, June 2004.

[8] Y. Su, S.B. Riffat, Y.L. Lin, and N. Khan, "Experimental and CFD study of ventilation flow rate of a Monodraught™ windcatcher," Energy and Buildings, vol. 40(6), pp. 1110-1116, December 2008.

[9] M.N. Bahadori, "Pressure coefficients to evaluate air flow pattern in wind towers," In International Passive and Hybrid Cooling Conference, American Section of the International Solar Energy Society, Miami Beach, Florida, pp. 206-210, November 1981.

[10] A.R. Dehghani-sanij, M. Soltani, and K. Raahemifar, "A new design of wind tower for passive ventilation in buildings to reduce energy consumption in windy regions," Renewable and Sustainable Energy Review, vol. 42, pp. 182-195, February 2015.

[11] L. Li, and C.M. Mak, "The assessment of the performance of a windcatcher system using computational fluid dynamics," Building and environment, vol. 42(3), pp. 1135-1141, March 2007.

[12] I. Janajreh and S. Emil, "Large eddy simulation of wind loads on a low-rise structure and comparison with wind tunnel results," Applied Mechanics and Materials, vol. 152, pp. 1806-1813, January 2012.

[13] I. Janajreh, "CFD Analysis of Wind Loads on Permeable Low-Rise Structures," Applied Mechanics and Materials, vol. 152, pp. 1814-1820, January 2012.

[14] V. Kalantar, "Numerical simulation of cooling performance of wind tower (Baud-Geer) in hot and arid region," Renewable Energy, vol. 34(1), pp. 246-254, January 2009.

[15] H. Saffari, and S.M. Hosseinnia, "Two-phase Euler-Lagrange CFD simulation of evaporative cooling in a Wind Tower," Energy and Buildings, vol. 41(9), pp. 991-1000, September 2009.

[16] I. Janajreh, K. Adouane and M. Hussain, "Wind Catcher and Trans-evaporative Cooling Residential Integration in Arid Region, Int. J. of Thermal & Environmental Engineering, Issue 1, vol. 14(1) , 2017.

[17]W.E. Ranz, and W.R. Marshall, "Evaporation from drops," Chemical Engineering Progress, vol. 48(3), pp. 141-146, March 1952.

[18] E.W. Peterson, and J.P. Hennessey Jr., "On the use of power laws for estimates of wind power potential," Journal of Applied Meteorology, vol. 17(3), pp. 390-394, March 1978.

[19] S.A. Hsu, E.A. Meindl, and D.B. Gilhousen, "Determining the power-law wind-profile exponent under near-neutral stability conditions at sea," Journal of Applied Meteorology, vol. 33(6), pp. 757-765, June 1994.

[20] I Janajreh, I Talab, "Wind data collection and analyses at Masdar City for wind turbine assessment", Int J. Ther Envi. Eng., vol. 1, 2010

[21] MR Hajj, IM Janajreh, HW Tieleman, TA Reinhold, "On frequency-domain analysis of the relation between incident turbulence and fluctuating pressures", Journal of wind engineering and industrial aerodynamics, vol 69, 1997